JOURNAL OF Applied Polymer SCIENCE

Improved Chemical Resistance of Ink-Jet Printed Micropatterns on Glass by Using Dual-Functional Compositions

Chi-Jung Chang, Hsin-Yu Tsai, Chih-Chiao Hsieh, Wei-Yun Chiu
Department of Chemical Engineering, Feng Chia University, Seatwen, Taichung 40724, Taiwan, Republic of China
Correspondence to: C.-J. Chang (E-mail: changcj@fcu.edu.tw)

ABSTRACT: UV curable and UV/moisture dual-functional oligomers were synthesized by grafting trimethoxysilane and methacrylate segments on the polyimide oligomer chains. These oligomers and a dual-functional monomer were used as ink compositions to enhance the chemical resistance of ink-jet printed LCD color filter micropatterns, without sacrificing jetting performance. The molecular structure and molecular weight of the oligomers were altered to adjust the solubility of oligomer in monomers, together with jetting trajectory, drop size uniformity, and deposition accuracy of the ink-jet inks. The chemical resistance, optical property, and mechanical property of the printed patterns depend on the oligomer structure, the arrangement of trimethoxysilane groups, and the molecular chain length. Straight lines and uniform dot arrays with excellent chemical resistance can be achieved. Dot patterns made of polymer-silica hybrid materials and pigments remain unchanged after being immersed in γ-butyrolactone for 200 min. © 2013 Wiley Periodicals, Inc. J. Appl. Polym. Sci. 130: 2049–2055, 2013

KEYWORDS: morphology; photopolymerization; coatings; dyes/pigments; mechanical properties

Received 6 February 2013; accepted 9 April 2013; Published online 14 May 2013
DOI: 10.1002/app.39396

INTRODUCTION

Polyimides possess excellent thermal stability and chemical resistance. In addition, the organic–inorganic hybrid nanocomposites provide unique properties, such as improved mechanical and thermal properties.[1–4] Thermal stability of the polymeric coatings can be improved by incorporating UV/moisture dual curable hyperbranched polyurethane. Besides, the hardness of the coating increased through the moisture curing process.[5] For the applications of organic–inorganic hybrid materials in optical device such as color filter, the inorganic domain should be smaller than the wavelength of the visible light and uniformly distributed within the hybrid material to achieve good mechanical properties and high transparency of the hybrid material.[6]

Ink-jet technology has been developed to eject the ink droplets to a specified position, which is important for sensor array,[7,8] organic light-emitting diodes,[9] color filter,[10] DNA microarray, and printed circuit board.[11–13] The performance of ink-jet printed pattern is dependent on the ink compositions. For example, the relationship between the dye/polymer/surfactant interaction and ink performance was investigated to design adequate ink composition for textile printing.[14] Fu et al.[15] reported that the printed fabrics with the pigmented ink containing core-shell latex exhibited high rub and washing fastness. Color filter is one of the important parts of the liquid crystal display. It consists of repeatedly arranged tiny red (R), green (G), and blue (B) pixels. At present, LCD CF is usually fabricated by the color photoresist process which requires three consecutive photolithography steps. Ink-jet printing process has the potential to reduce the fabrication cost of color filter.[16–20] Chen[21] reported the fabrication of an ink-jet printed stripe-type LCD color filter. Micrometer sidewalls were used as barriers in their process to prevent color mixing problem. To fix the pattern on glass substrate after ink-jet printing, curing reaction is necessary to quickly convert the low-viscosity liquid inks pattern into a solid polymer network. Color filter (CF) should exhibit good transmittance, high-temperature durability, and chemical resistance. For the fabrication of liquid crystal displays, the alignment-film is coated on the color filter. The color stripes should not be peeled off or be dissolved in the solvent during the cleaning process and alignment-film coating processes. The printed micropatterns should exhibit good solvent resistance. Besides, the adhesion between the pattern and the glass substrate should be good enough. γ-butyrolactone is commonly used for the chemical resistance tests.

In this study, patterns were ink-jet printed by the nonvolatile inks which contain no solvent. No color wells or side wall is necessary in this process. The RGB pixels can be formed in a single step by ejecting the ink drops onto the color areas and fixing the pattern through curing reaction. Chemical resistance of the cured pattern was evaluated by comparing the solvent

immersion time of the cured dot patterns that the printed dots remained unchanged. In our previous study,[22] hyperbranched polyurethane-methacrylates were synthesized and used as oligomers for ink-jet printing of LCD color filters. Printed dots were not dissolved or peeled off after being immersed in γ-butyrolactone for 20 min. The goal of this study is to make ink-jet printed micropatterns on glass with better solvent resistance than that reported in our previous study.[22] Our strategy is to fix the pattern by UV curing and moisture curing after ink-jet printing. UV/moisture curable oligomers were prepared by grafting UV-curable segments and alkoxylsilane segments on the polyimide chains. Two UV curable oligomers with different molecular weight, dual curable oligomer, and monomer were used as ink compositions. In this study, dot patterns made of polymer–silica hybrid materials and pigments remain unchanged after being immersed in γ-butyrolactone for 200 min. The effects of moisture curing moiety and molecular chain length of curable compositions on the chemical resistance, optical property, and mechanical property of the printed patterns were investigated.

EXPERIMENTAL

Materials

2,2-Bis(3-amino-4-hydroxyphenyl)hexafluoropropane (M3) was purchased from Chriskev. 2-ethyl-4-methylimidazole (2,4-EMI) and 3-glycidoxypropyl trimethoxysilane (TGS) were supplied by Acros. 5-(2,5-Dioxotetrahydrofuryl)-3-methyl-3-cyclohexene-1,2-dicarboxylic anhydride (H2) was purchased from Alfa Aesar. 2,2-Bis(4-(4-aminophenoxy)-phenyl) hexafluoropropane (M6), triphenylphosphine (TPP), 2-(methacryloyloxy)ethyl isocyanate (MEI), and 3-(trimethoxysilyl)propyl methacrylate (TMS) were supplied by TCI. Glycidyl methacrylate (GMA) was purchased from Aldrich. Pentaerythritol triacrylate (PETA) and tripropylene glycol diacrylate (TPGDA) were provided by Sartomer. The catalyst dibutyltin dilaurate (DBTDL) was supplied by Alfa Aesar. Surfactant BYK333 was provided by BYK Gardner.

Preparation of Soluble Polyimides

Dianhydride H2 is purified by recrystallization from acetic anhydride and then dried in a vacuum oven at 120°C overnight. The polyamic acid (PAA) solutions are made by reacting dianhydride H2 (1 mmol) with diamine M3 (0.5 mmol) and diamine M6 (0.5 mmol) in DMF under a nitrogen atmosphere and stirring for 12 h. The solid content is 20 wt %. Then, pyridine and ethanoyl ethanoate were added in the PAA solution. The solution was reacted at 130°C for 3 days under a nitrogen atmosphere. After cooling, the solution was poured into excess D.I. water and filtered. The process repeated three times. Soluble PIS (PIL) were obtained after drying. PIS was prepared by similar procedure except the soluble polyimides (PI) were synthesized by half amount of dianhydride (H2). The symbols L and S represent the polyimides with larger and smaller molecular weight, respectively.

Preparation of UV Curable Polyimides (PIL-M and PIS-M)

Soluble PI (PIL), MEI, and the catalyst DBTDL were dissolved in DMF. The solution was reacted at 40°C for 24 h. After cooling, PIL-M can be obtained by washing with excess methanol and drying. PIS-M was prepared by similar procedure except the soluble polyimides PIL was replaced by PIS. PIL-M and PIS-M represent the UV curable polyimides with larger and smaller molecular weight, respectively.

Preparation of Dual-Functional Polyimides (PIL-GT)

The soluble polyimides PIL, catalysts TPP, and 2,4-EMI were dissolved in DMF. Then, GMA and TGS were added into the solution. The solution was reacted at 70°C for 72 h under a nitrogen atmosphere. After cooling, it was washed with excess ethyl ether and dried to make PIL-GT. The reaction scheme is listed in Figure 1.

Preparing for UV-Curable Ink-Jet on Printing

Red pigment concentrate was dispersed in monomer TPGDA. Then, pentaerythritol-triacrylate monomer, photoinitiator 2-hydroxy-2-methyl-1-phenyl-propan-1-one, surfactant BYK333, and the as-synthesized curable polyimide were added in the previous dispersion and stirred for 3 h. The mixture was passed through a 0.22 μm filter to make the curable ink-jet ink. Curable polyimide acted as an oligomer in the ink. In this study, various oligomers and dual functional monomer have different solubility in the ink. They were added as much as it can be dissolved in the ink. The UV curable ink-jet inks were prepared according to the formula listed in Table I.

Ink-Jet Printing

An ink-jet printer equipped with a Xaar-128 piezo print head was used to print the micropattern. The printed pattern was then fixed by curing reactions. All the jetting properties were measured by a high-speed image capture system (resolution: 5 μs). The system consists of a cartridge holder, a light emitting diode (LED), a zoom lens, a CCD camera, and a signal control device. The signal control device can be utilized to adjust the flashing signal of the LED, along with the operating parameters of the cartridge such as the applied voltage, pulse width, firing frequency, and delay time. The jetting frequency is 3000 Hz.

Characterization

All the jetting properties were measured by the high-speed image-capture system.[23] To evaluate the mechanical properties of the cured films, these were subjected to a nanoindentation test that used a Nanotest (Micromaterials) nanoindentor. The load was applied to the surface with an 8-s hold period at a maximum applied load of 5.35 mN. ^{29}Si NMR spectra were recorded with a Bruker DSX400WB (400 MHz) NMR spectrometer. The viscosity and surface tension of the inks were investigated by Brookfield DV-II viscometer and Kruss K6 tensiometer. The particle sizes of the inks were measured by Beckman Coulter N4 plus laser diffraction submicron particle size analyzer.

RESULTS AND DISCUSSION

FTIR Spectra of Oligomers

In Figure 2(a), FTIR spectrum of 2-isocyanatoethyl methacrylate (MOI) exhibits an absorption peak of the isocyanato group at 2261 cm^{-1}. The peak of the isocyanato groups of the PIL-M [Figure 2(b)] disappeared at the end of the reaction. The peak at 1720 cm^{-1} is attributed to carbonyl groups of urethano units (–HNCOO–). It gradually increases with the decrease of the

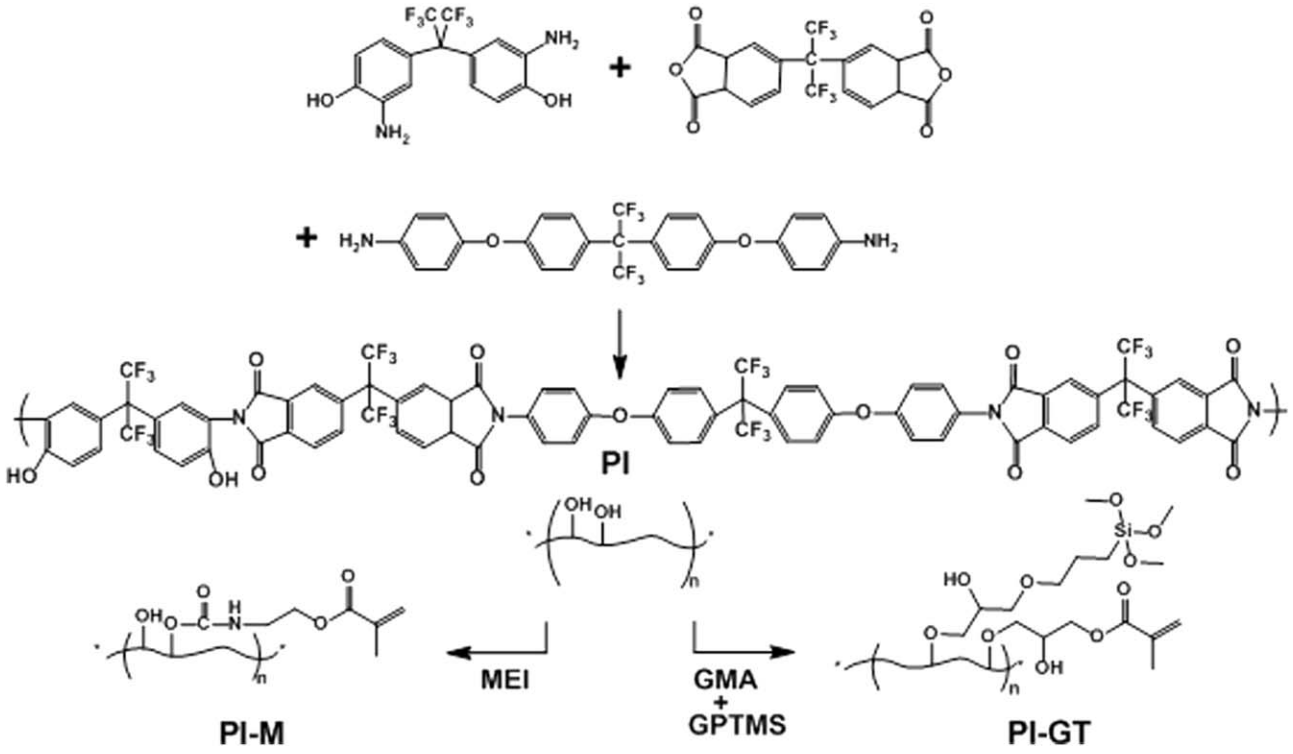

Figure 1. Synthesis of PI-M series UV curable oligomers and dual-functional oligomer PI-GT.

absorption peak of isocyanato groups. The peak at 1540 cm^{-1} is attributed to the formation of –CNH– linkage. These results confirm the formation of PIL-M oligomer.

The IR spectrum of the mixture of soluble polyimides PIL, reactants GMA, and TGS is shown in Figure 2(c). After reacting at 70°C for 72 h, the absorption peak at 910 cm^{-1} (oxirane ring of GMA and TGS) disappeared, as shown in Figure 2(d). The product is the PIL-GT oligomer.

Drop Formation Properties of Inks

When a high-molecular-weight polymer is used as ink composition, the fluid filament will connect with the nozzle and no separate drops will be observed.[24] To get separated drops with good jetting performance during the jet-printing process, the molecular weight (M_n) of the oligomer is controlled bellow 12,000 in this study. Figure 3 shows the drop formation images of PIL-M, PIS-M, PIL-GT, and TMS inks captured at different delay time. The delay time was the time interval between the jetting signal triggering and the image capture operation. The focus of the zoom lens was adjusted to a selected nozzle. If the delay time is set at 20 μs, an image was captured after the drop was ejected for 20 μs. The ejected ink drops of PIL-M, PIS-M, PIL-GT, and TMS inks exhibit straight trajectory. However, the drop velocities of these inks are different. The drop velocities of PIL-M, PIS-M, PIL-GT, and TMS inks are 2.5, 2.1, 1.9, and 3.7 m/s, respectively. Properties of inks and jetted drops were illustrated in Table II. The drop velocity of the PIL-M inks reaches 2.5 m/s. Because of the higher solubility of PIS-M oligomer, more PIS-M oligomer is added in ink than its high molecular weight analog PIL-M. Viscosity of PIS-M ink is higher than that of PIL-M ink. The drop velocity of the PIS-M ink is slower than that of the PIL-M ink. Similar result was also found in the drop formation images of the PIL-GT ink. The drop velocity of the PIL-GT ink is even slower. The molecular chain length of TMS is smaller than those of the other three oligomers. Although TMS content in ink reached 10%, the viscosity of TMS ink were lower than those of PIS-M and PIL-GT inks. The drop velocities of TMS ink is the highest among the four inks.

Table I. Compositions of the Ink-Jet Inks with Different Curable Materials

Ink	Tripropylene glycol diacrylate (TPGDA) (wt %)	Pentaerythritol triacrylate (PETA) (wt %)	Oligomer or monomer (wt %)
PIL-M	72.14	10.00	0.36 (PIL-M)
PIS-M	71.08	10.00	1.42 (PIS-M)
PIL-GT	71.10	10.00	1.40 (PIL-GT)
TMS	62.50	10.00	10.00 (TMS)

Photoinitiator (2-hydroxyl-2-methyl-1-phenyl- propan-1-one): 2 wt %.
Surfactant (Byk333): 0.5%.
Pigment dispersion: 15 wt %.

Deposition Accuracy, Uniformity, and Chemical Resistance of Printed Dots

Properties printed micropatterns were illustrated in Table II. A dot-matrix test pattern was designed to check the jet-printing performance such as jetting trajectory and drop size uniformity. The printed and UV-cured dots of the PIL-M, PIS-M, PIL-GT, and TMS inks on the glass substrate are shown in Figure 4(a,d,h,*l*), respectively. To make color stripe pattern with

Applied Polymer SCIENCE

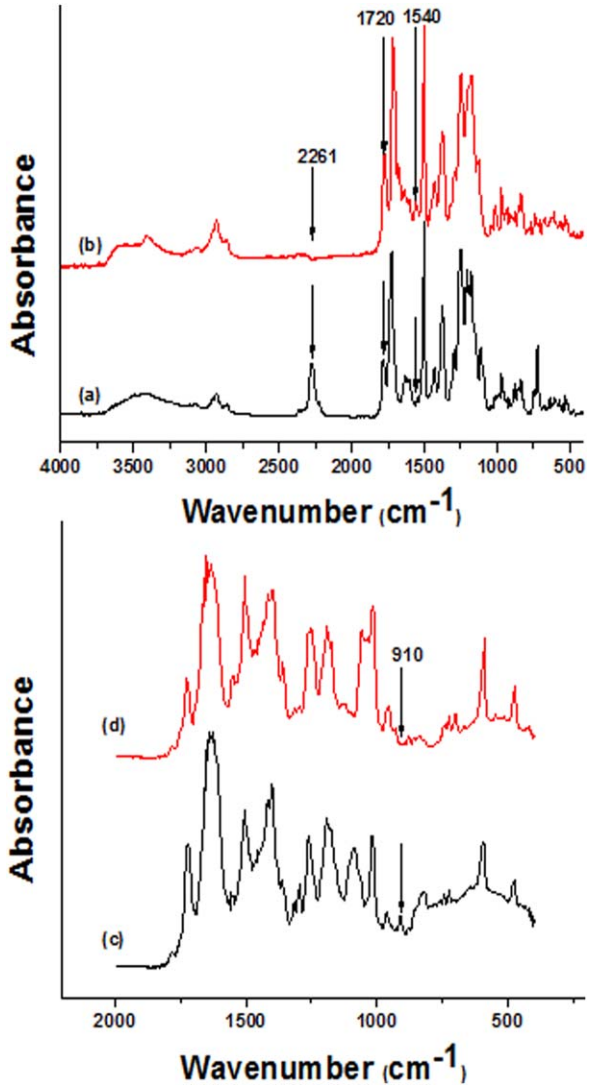

Figure 2. FTIR spectra of (a) the mixture of PIL and MOI, (b) PIL-M oligomer, (c) the mixture of PIL, GMA, and TGS, and (d) PIL-GT oligomer. [Color figure can be viewed in the online issue, which is available at wileyonlinelibrary.com.]

straight and sharp edges, the printing dots should exhibit good deposition accuracy and uniform drop size. Then, the printing parameters of the ink-jet CF printer, such as the number of ink drops to be ejected within a certain distance, can be determined to make good CF patterns. The PIL-M [Figure 4(a)], PIS-M [Figure 4(d)], PIL-GT [Figure 4(h)], and TMS [Figure 4(l)] inks exhibit straight trajectory. The printed dots in the dot matrices of these inks are well aligned. There are no large displacements which may lead to some error dots lying in the neighboring stripes. All dots of the same ink showed almost the same size. It reveals that the drop volume of each ejected ink drop is about the same. The average sizes of dots printed by PIL-M, PIS-M, and PIL-GT inks are 130.5 ± 1.7, 129.8 ± 2.4, 129.8 ± 1.6 μm, respectively. However, the average size of TMS dot is much larger than those of the other three.

Figure 4 also shows the OM images of dots of PIL-M ink, PIS-M ink, PIL-GT ink, and TMS ink immersed in butyrolactone solvent for different period of time. The chemical resistance of different cured patterns was investigated by comparing images of the cured dot patterns after being immersed in γ-butyrolactone. For dots prepared by the PIL-M ink, some dots were completely peeled away after being immersed in γ-butyrolactone for 20 min. More PIL-M dots were removed as the immersion time increased to 40 min. Dots prepared by the PIS-M ink remained the same after being immersed in γ-butyrolactone for 40 min. When the immersion time extended to 200 min, some dots were completely removed. The PIS-M dots have better chemical resistance than the PIL-M dots. The molecular weight of PIL-M oligomer is higher than its analog PIS-M. The solubility of the PIS-M oligomer in monomers is higher than that of the PIL-M oligomer. As shown in the formulation table, compared with PIL-M oligomer (0.36 wt %), more PIS-M oligomer (1.42 wt %) can be added in the ink. Dots prepared by the PIL-GT and TMS inks remained the same after being immersed in γ-butyrolactone for 200 min. The PIL-GT and TMS dots exhibit the best chemical resistance among the four inks. The oligomer contents of PIS-M and PIL-GT inks are about the same. The alkoxylsilane groups on the side chains of PIL-GT oligomers may play an important role. As illustrated in Figure 5, after ink-jet printing, the UV curing reaction of acrylate segments, and the gelation reaction of the hydrolyzed alkoxylsilane occurred simultaneously. The alkoxylsilane groups on the oligomers can react with the surface functional groups on glass through the sol–gel reactions. Such reaction may enhance the adhesion between the printed micropatterns and the glass substrate during solvent immersion. That may explain why the PIL-GT and TMS ink exhibits excellent chemical resistance.

Si-NMR Spectra

^{29}Si NMR spectroscopy provides information about the type of connecting bonds.[25] Tri-functional silicon sites are labeled with the T^n notation. The superscript n denotes the number of siloxane bonds.[26] To illustrate the silica structures formed in the hybrid films, the peak integrations were collected by setting the deconvolution assignments at −44 ppm (T^0), −50 ppm (T^1), −59 ppm (T^2), and −67 ppm (T^3). Figure 6 shows the ^{29}Si-NMR spectrum of the cured TMS ink. The degree of condensation of the silane groups can be determined by calculating the integration of the ^{29}Si NMR peaks at fixed chemical shift regions using the following equation.[27] The degree of condensation of the Si–OH condensation reactions in the TMS hybrid film is 7.5%. It confirms the formation of siloxane bonds in the cured hybrid materials.

$$\text{Degree of condensation} = \frac{T^1 + 2T^2 + 3T^3}{3(T^0 + T^1 + T^2 + T^3)} \times 100$$

Since silica was formed by the sol–gel reaction of adjacent silane groups, monomer concentration, and silane group arrangement in monomers/oligomers may have great influences on the properties of cured hybrid composites. Dual functional monomer TMS has higher solubility in ink than the dual functional oligomer PIL-GT. Various oligomer and dual functional monomer were added as much as they can be dissolved in the ink. The content of TMS in ink (10 wt %) is about 7 times of PIL-GT in ink (1.4 wt %). For the PIL-GT film, only T^0 peak is

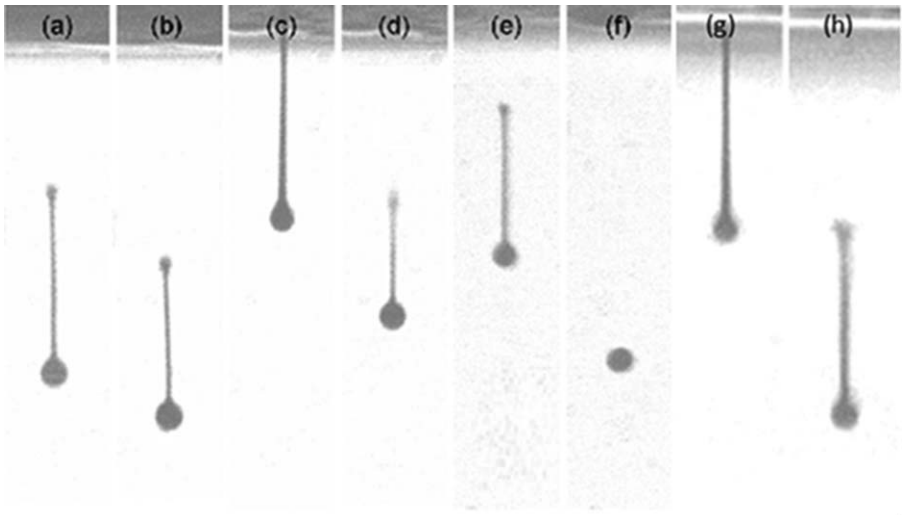

Figure 3. Drop formation images of inks captured at different delay times: PIL-M ink: (a) 20 μs, (b) 40 μs; PIS-M ink: (c) 20 μs, (d) 100 μs; PIL-GT ink: (e) 20 μs, (f) 90 μs; TMS ink: (g) 20 μs, and (h) 80 μs.

observed in ^{29}Si NMR spectrum. The amount of reacted silane groups was not detectable. Sol–gel reaction of adjacent silane groups is restricted because of the low concentration and limited molecular chain mobility of PI oligomer. For the TMS hybrid film, transformation of the molecular structure was observed with decreasing T^0, and increasing T^1 in ^{29}Si NMR spectrum. The content of TMS in ink reached 10 wt %. Shorter TMS monomer chain and higher TMS content in ink may help the sol–gel reaction of silane groups on adjacent TMS monomers.

Morphology of Printed Stripes

The OM images of the red stripes printed by the PIL-M, PIS-M, PIL-GT, and TMS inks are shown in Figure 7. Properties of printed micropatterns were illustrated in Table II. The line width is larger than the diameter of the jetted drop (before reaching the substrate). It may result from the wetting of inks and the coalescence of adjacent drops. PIL-M stripes [Figure 7(a)] show straight edges and good color uniformity. However, the compatibility problem between the PIS-M oligomer and the pigment deteriorate the printing quality. There are two deep red spots resulting from the coagulation of pigment found in the PIS-M stripes [Figure 7(b)]. PIL-GT stripes [Figure 7(c)] exhibit good color uniformity. The average line widths of PIL-M, PIS-M, and PIL-GT stripes are 136.3 $\pm$ 2.1, 137.1 $\pm$ 3.8, and 139.4 $\pm$ 3.6 μm, respectively. The average line width of TMS stripe is much larger than those of the other three. Although PIL-M and PIS-M stripes exhibited straight edge and good uniformity, micropatterns printed by TMS and PIL-GT inks had much better chemical resistance than those printed by PIL-M and PIS-M inks (Figure 4). Considering the chemical resistance and line width of the printed patterns, PIL-GT ink is preferred for the fabrication of high resolution micropatterns on glass substrates.

Nanoindentation Properties of Printed Stripes

The mechanical properties of the printed stripes were investigated by the nanoindentation test. Load and penetration depth were simultaneously monitored during both loading and unloading periods, to obtain the force-depth diagram. The diagram revealed the elastic and plastic deformations with increasing load. Figure 8 shows the force-depth plots of the UV-cured PIL-M, PIS-M, PIL-GT, and TMS films during the nanoindentation tests. The hardnesses of PIL-M and PIS-M films are 0.11 and 0.14 GPa, respectively. In Table I, PIS-M oligomer exhibits higher solubility in monomers than its analog PIL-M does. The hardness of the PIS-M film prepared by inks with PIS-M oligomer is higher than that of the PIL-M film. For the films prepared by dual-functional compositions, the hardnesses of PIL-GT and TMS films are 0.12 and 0.17 GPa, respectively. The modulus of PIL-GT and TMS films are 4.50 and 7.15, GPa respectively. In the "Si-NMR Spectra" section, for the TMS hybrid film, condensation of the Si–OH condensation reactions

Table II. Properties of Inks, Jetted Drops, and Printed Micropatterns of Inks with Different Oligomers or Monomers

	Ink jet inks			Jetted drops		Printed micropatterns			
Inks	Viscosity (cps)	Surface tension (mN/m)	Average particle size (nm)	Drop velocity (m/s)	Drop diameter (μm)	Dot diameter (μm)	Lines width (μm)	Hardness (GPa)	Modulus (GPa)
PIL-M	13.1	40.2	41.6	2.5	89	130.5	136.3	0.11	4.08
PIS-M	15.8	39.5	28.8	2.1	89	129.8	137.1	0.14	4.25
PIL-GT	15.4	39.2	24.6	1.9	78	129.8	139.4	0.12	4.50
TMS	13.5	38.1	30.2	3.7	100	223.5	225.0	0.17	7.15

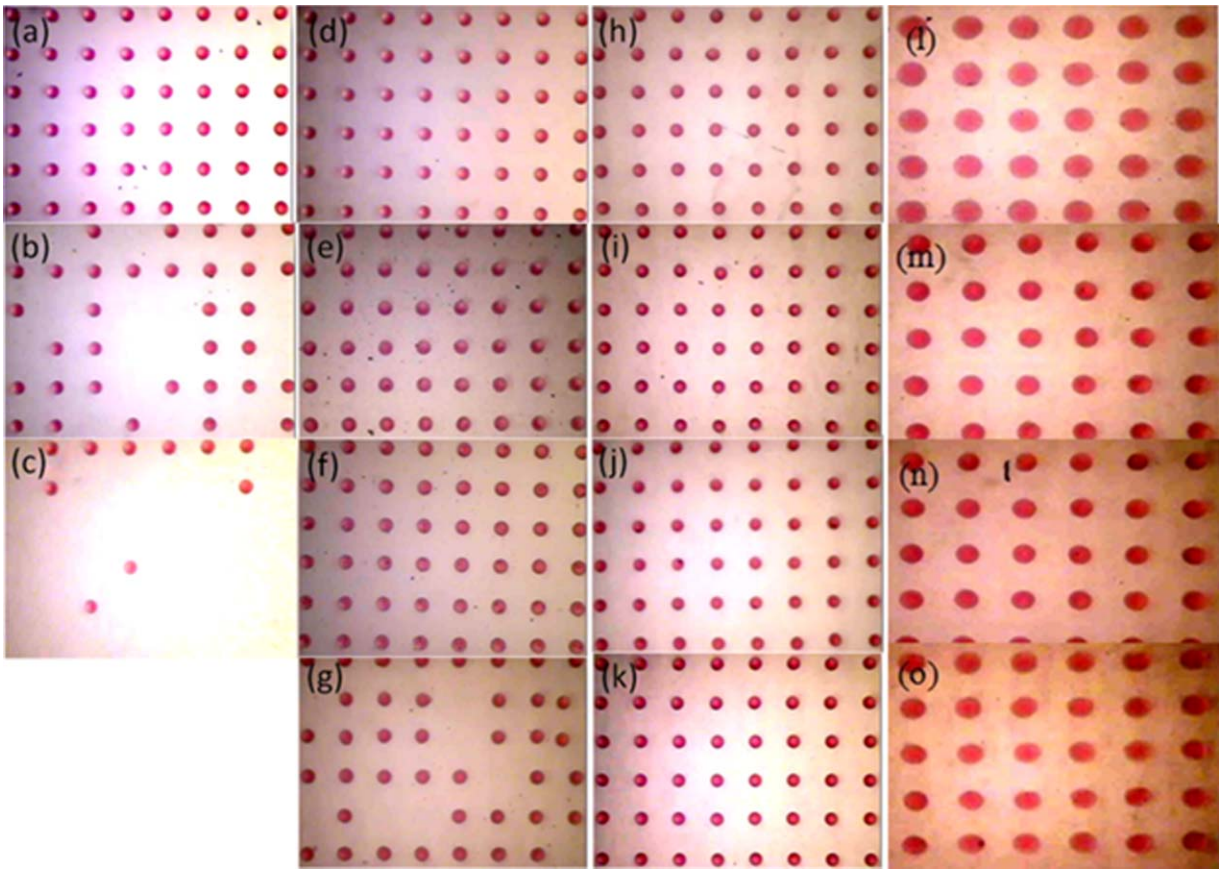

Figure 4. OM images of dots of PIL-M ink (a) printed/cured and immersed in butyrolactone solvent for (b) 20 min, (c) 40 min; dots of PIS-M ink (d) printed/cured and immersed in butyrolactone solvent for (e) 20 min, (f) 40 min, (g) 200 min; dots of PIL-GT ink (h) printed/cured and immersed in butyrolactone solvent for (i) 20 min, (j) 40 min, (k) 200 min; dots of TMS ink (l) printed/cured and immersed in butyrolactone solvent for (m) 20 min, (n) 40 min, (o) 200 min. [Color figure can be viewed in the online issue, which is available at wileyonlinelibrary.com.]

was observed with decreasing T^0, and increasing T^1 in ^{29}Si NMR spectrum. Shorter TMS monomer chain and higher TMS content in ink help the sol–gel reaction of silane groups on adjacent TMS monomers. It leads to the increase in hardness and modulus of the TMS film through the moisture curing process.

CONCLUSION

Two UV curable oligomers with different molecular weights, and a dual-functional polyimide oligomer with UV-curable acrylate segments and moisture-curable alkoxylsilane segments were synthesized and used as ink compositions to improve the chemical resistance of the printed pattern on glass. Without using side wall, ink-jet printed lines with straight edge and good color uniformity, together with precisely printed dot array

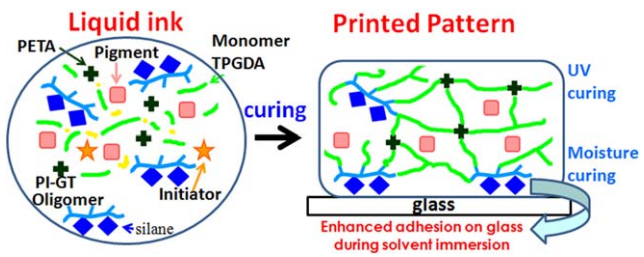

Figure 5. Illustration of the curing reaction for printed pattern and enhanced adhesion between the pattern/glass interface by the sol–gel reaction. [Color figure can be viewed in the online issue, which is available at wileyonlinelibrary.com.]

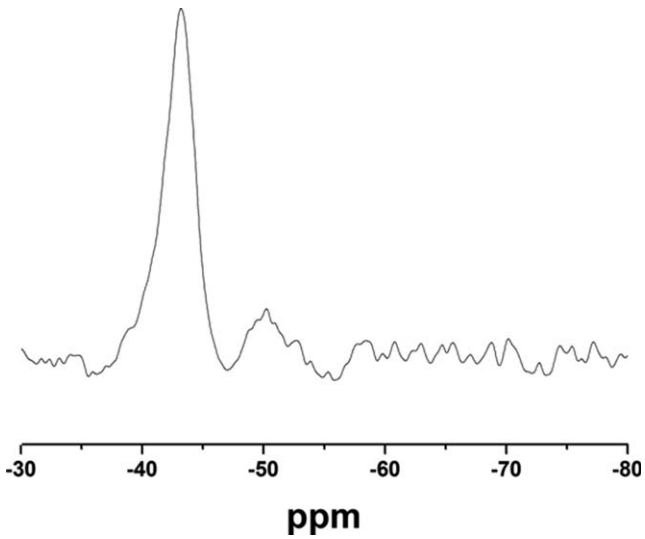

Figure 6. ^{29}Si-NMR spectrum of the cured TMS ink.

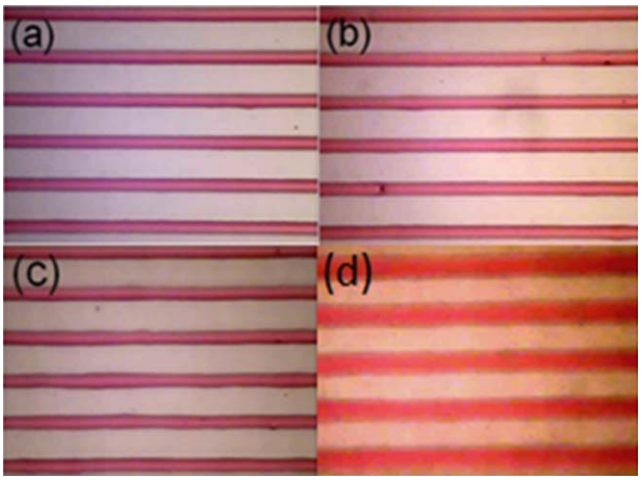

Figure 7. OM images of lines printed by (a) PIL-M, (b) PIS-M, (c) PIL-GT, and (d) TMS inks. [Color figure can be viewed in the online issue, which is available at wileyonlinelibrary.com.]

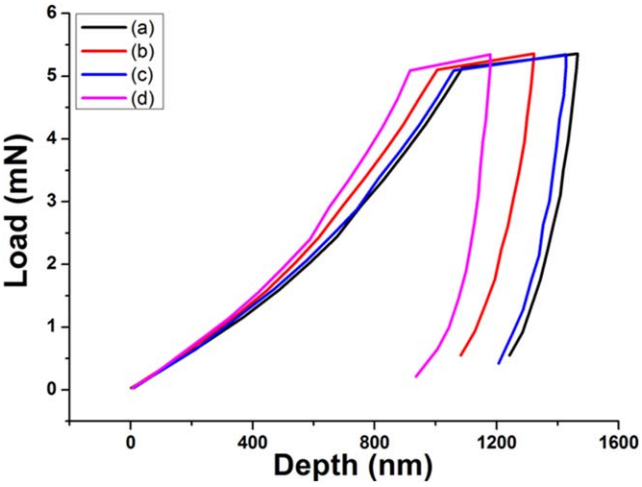

Figure 8. Force-depth plots of the films prepared by inks using (a) PIL-M, (b) PIS-M, (c) PIL-GT, and (d) TMS oligomers during the nanoindentation tests. [Color figure can be viewed in the online issue, which is available at wileyonlinelibrary.com.]

can be obtained. The chemical resistance and mechanical property of the printed patterns were improved by introducing the moisture curing moiety and changing molecular chain length of curable compositions. The organic–inorganic hybrid color patterns made by inks with dual curable oligomer or monomer showed better chemical resistance than their analogs using UV curable oligomers. Dots prepared by the PIL-GT and TMS inks remained the same after being immersed in g-butyrolactone for 200 min. However, PIL-GT ink is preferred for the fabrication of high resolution micropatterns on glass substrates.

ACKNOWLEDGMENTS

The authors would like to thank the financial support from National Science Council under the contract of NSC-98-2221-E-035-003. The authors appreciate the Precision Instrument Support Center of Feng Chia University in providing the measurement facilities.

REFERENCES

1. Zhu, J.; Morgan, A. B.; Lamelas, F. J.; Wikkie, C. A. *Chem. Mater.* **2001**, *13*, 3774.
2. Tsai, M. H.; Chang, C. J.; Chen, P. J.; Ko, C. J. *Thin Solid Films* **2008**, *516*, 5654.
3. Matejka, L.; Dukh, O.; Kolarik, J. *Polymer* **2000**, *41*, 1449.
4. Chang, C. J.; Wu, M. S.; Kao, P. C. *J. Polym. Sci. Part B: Polym. Phys.* **2007**, *45*, 1152.
5. Liang, H.; Hao, M. ; Guan, J.; Xiong, L.; Zhong, W. *Acta Polym. Sinica* **2009**, *12*, 1211.
6. Chang, C. J.; Tzeng, H. Y. *Polymer* **2006**, *47*, 8536.
7. Li, B.; Santhanam, S.; Schultz, L.; Jeffries-EL, M.; Iovu, M. C.; Sauve, G.; Cooper, J.; Zhang, R.; Revelli, J. C.; Kusne, A. G.; Snyder, J. L.; Kowalewski, T.; Weiss, L. E.; McCullough, R. D.; Fedder, G. K. ; Lambeth, D. N. *Sens. Actuators B* **2007**, *123*, 651.
8. Chang, C. J. ; Hung, S. T.; Lin, C. K.; Chen, C. Y.; Kuo, E. H. *Thin Solid Films* **2010**, *519*, 1693.
9. Ding, Z.; Xing, R.; Fu, Q.; Ma, D.; Han, Y. *Org. Electron.* **2011**, *12*, 703.
10. Chang, C.J.; Shih, K.C.; Chang, S.J.; Wu, F.M.; Pan, F.L. *J. Polym. Sci. Part B: Polym. Phys.* **2005**, *43*, 3337.
11. Moon, K. S.; Choi, J. H.; Choi, D. J. ; Kim, S. H.; Ha, M. H.; Nam, H. J.; Kim, M. S. *J. Micromech. Microeng.* **2008**, *18*, 125011.
12. Goldmann, T.; Gonzalez, J. S.; *Biochem. J. Biochem. Biophys. Methods* **2000**, *42*, 105.
13. Kim, C. S.; Park, S. J.; Sim, W. C.; Kim, Y. J.; Yoo, Y. S. *Comput. Fluids* **2009**, *38*, 602.
14. Park, J. Y.; Hirata, Y.; Hamada, K. *Dyes Pigments* **2012**, *95*, 502.
15. Fu, S.; Tian, A.; Du, C.; Wang, C. *J. Appl. Polym. Sci.* **2013**, *127*, 2678.
16. Rudin, J.; Kitson, S.; Geisow, A. *SID'08 Dig.* **2008**, 641.
17. Chang, C. J.; Tsai, M. H.; Kao, P. C.; Tzeng, H. Y. *Thin Solid Films* **2008**, *516*, 5503.
18. Chang, C. J.; Wu, F. M.; Chang, S. J.; Hsu, M. W. *Jpn. J. Appl. Phys.* **2004**, *43*, 6280.
19. Chang, C. J.; Chang, S. J.; Wu, F. M.; Hsu, M. W.; Chiu, W. W.; Cheng, K. *Jpn. J. Appl. Phys.* **2004**, *43*, 8227.
20. Koo, H. S.; Pan, P. C.; Kawai, T.; Chen, M.; Wu, F. M.; Liu, Y. T.; Chang, S. *J. Appl. Phys. Lett.* **2006**, *88*, 111908.
21. Chen, C. T.; Wu, K. H.; Lu, C. F.; Shieh, F. *J. Micromech. Microeng.* **2010**, *20*, 055004.
22. Chang, C. J.; Lin, Y. H. ; Tsai, H. Y. *Thin Solid Films* **2011**, *519*, 5243.
23. Chang, C. J.; Chang, S. J.; Tsou, S.; Chen, S. I.; Wu, F. M.; Hsu, M. W. *J. Polym. Sci. Part B: Polym. Phys.* **2003**, *41*, 1909.
24. Gans, B. D.; Duineveld, P. C.; Schubert, U. S. *Adv. Mater.* **2004**, *16*, 203.
25. Kim, S. Y.; Augustine, S.; Eo, Y. J.; Bae, B. S.; Woo, S. I.; Kang, J. K. *J. Phys. Chem. B* **2005**, *109*, 9397.
26. Sepeur, S.; Kunze, N.; Werner, B.; Schmidt, H. H. *Thin Solid Films* **1999**, *351*, 216.
27. Kim, W. S.; Houbertz, R.; Lee, T. H.; Bae, B. S. *J. Polym. Sci. Part B: Polym. Phys.* **2004**, *42*, 1979.